EPJ manuscript No.
(will be inserted by the editor)

Deuteron and triton production with high energy sulphur and lead beams

I.G. Bearden[1], H. Bøggild[1], J. Boissevain[2], P.H.L. Christiansen[1], L. Conin[4], J. Dodd[3], B. Erazmus[4], S. Esumi[5], C.W. Fabjan[6], D. Ferenc[7a], A. Franz[6b], J.J. Gaardhøje[1], A.G. Hansen[1c], O. Hansen[1], D. Hardtke[9d], H. van Hecke[2], E.B. Holzer[6], T.J. Humanic[9], P. Hummel[6], B.V. Jacak[10], K. Kaimi[5e], M. Kaneta[5d], T. Kohama[5], M. Kopytine[10f], M. Leltchouk[3], A. Ljubičić Jr.[7b], B. Lörstad[11], L. Martin[4], A. Medvedev[3], M. Murray[8], H. Ohnishi[5b], G. Paić[6,9], S.U. Pandey[9], F. Piuz[6], J. Pluta[4g], V. Polychronakos[12], M. Potekhin[3], G. Poulard[6], D. Reichhold[9h], A. Sakaguchi[5i], J. Schmidt-Sørensen[11], J. Simon-Gillo[2j], W. Sondheim[2], T. Sugitate[5], J.P. Sullivan[2], Y. Sumi[5k], W.J. Willis[3], K. Wolf[8e], N. Xu[2d], and D.S. Zachary[9]

[1] Niels Bohr Institute, DK-2100 Copenhagen, Denmark.
[2] Los Alamos National Laboratory, Los Alamos, NM 87545, USA.
[3] Department of Physics, Columbia University, New York, NY 10027,USA.
[4] Nuclear Physics Laboratory of Nantes, 44072 Nantes, France.
[5] Hiroshima University, Higashi-Hiroshima 739-8526, Japan.
[6] CERN, CH-1211 Geneva 23, Switzerland.
[7] Rudjer Bošković Institute, Zagreb, Croatia.
[8] Cyclotron Institute, Texas A&M University, College Station, TX 77843, USA.
[9] Department of Physics, The Ohio State University, Columbus, OH 43210, USA.
[10] State University of New York, Stony Brook, NY 11973, USA.
[11] Department of Physics, University of Lund, S-22362 Lund, Sweden.
[12] Brookhaven National Laboratory, Upton, NY 11973, USA.

Received: date / Revised version: date

Abstract. Proton and deuteron production has been observed in S+S and S+Pb collisions at 200 A·GeV and in Pb+Pb reactions at 158 A·GeV at the CERN SPS accelerator. For Pb+Pb triton production was also measured. The p and d spectra as well as the p and t spectra were observed in similar rapidity ranges and over similar ranges of transverse momenta per nucleon, making it possible to interpret the cross sections of the composite particles in terms of coalescence mechanisms. Volumes of homogeneity were extracted and compared to pion-pair HBT interferometry results. Special attention is given to the dependence on transverse mass, centrality and rapidity.

PACS. PACS-key

1 Introduction

The present paper reports on measurements of transverse momentum spectra of protons, deuterons and tritons from Pb+Pb collisions at 158 A·GeV/c beam momentum and for S+Pb and S+S at 200 A·GeV/c. The measurements were made in approximately the same range of transverse momenta per nucleon for all three species (p, d and t) and in similar rapidity intervals. The data therefore readily lend themselves to an analysis in terms of the nucleon [1–4] or fragment [5] coalescence models. Such an analysis leads to estimates of the reaction volume at freeze-out (i.e. at a time when strong interactions between the final state hadrons have ceased).

Deuterons and tritons are fairly large objects compared to simple hadrons and their binding energies (2.2 and 8.2 MeV, respectively) are small compared to freeze-

[a] now at University of California, Davis, CA 95616, USA
[b] now at BNL, Upton, NY 11973, USA.
[c] now at LANL, Los Alamos, NM 87545, USA.
[d] now at LBNL, Berkeley,CA 94720, USA
[e] deceased
[f] On unpaid leave from P.N.Lebedev Physical Institute, Russian Academy of Sciences.
[g] now at Institute of Physics, Warsaw University of Technology, Koszykowa 75,00-662, Warsaw, Poland.
[h] now at Creighton University, Omaha, NE 68178, USA.
[i] now at Osaka University, Toyonaka, Osaka 560-0043, Japan.
[j] now at U.S. Department of Energy, Germantown, MD 20874-1290, USA.
[k] now at Hiroshima International University, 555-36 Kurosecho, Hiroshima 724-0695, Japan

out temperatures, which are on the order 100 MeV. These light clusters are therefore not expected to survive through the high density stages of the collision. The deuterons and tritons observed in the experiment are formed and emitted near freeze-out, and they mainly carry information about this late stage of the collision. This is evident from the simple nucleon coalescence model [3,4], where the light cluster A(Z,N) is formed with an invariant multiplicity density in momentum space

$$E_A \frac{d^3N_A}{dp_A^3} = B_A (E_p \frac{d^3N_p}{dp_p^3})^A, \quad (1)$$

where the cluster momentum $p_A = Ap_p$ and p_p is the nucleon momentum, and it has been assumed that the neutron momentum density is proportional to the proton momentum density at freeze-out. The coalescence factor B_A can be derived from the measured invariant cross sections and it may be related to a freeze-out (source) volume V under conditions of thermodynamical equilibrium (thermal and chemical equilibrium),

$$B_A = A \frac{2s_A + 1}{2^A} R_{np}^N (\frac{h^3}{m_p \gamma V})^{A-1}. \quad (2)$$

Here R_{np} is the ratio of neutrons to protons participating in the collision, γ is the the Lorentz factor related to the velocity β of the cluster A(Z,N) by $\gamma = 1/\sqrt{1-\beta^2}$. Eq.(2) is valid only in the limit of the cluster binding energy being much smaller than the freeze-out temperature and for clusters that have no bound excited states.

The experiments presented here pay special attention to the transverse mass (m_t) and rapidity dependence of the measured B_A-values. The observed m_t-dependence, in particular, shows that the simple thermodynamic expression eq.(2) is not the proper model for an interpretation of the data; instead more complicated models that include collective flow explicitly [6–9] must be invoked. Under the conditions of special flow patterns Scheibl and Heinz [9] have derived an extension of eq.(2) that allows the comparison of interaction volumes or rather "lengths (or volumes) of homogeneity" derived from Hanbury-Brown, Twiss (HBT) interferometry, with similar volumes derived from cluster formation cross sections. Such an analysis is presented for the Pb+Pb case at a nucleon transverse mass of ≈1 GeV, and good agreement between the volumes of homogeneity from interferometry and coalescence is demonstrated. The observed dependence of B_2 on rapidity, however, disagrees with the model of Ref. [9]. Finally, an analysis of the triton formation by coalescence is presented, also in terms of the models of Refs. [6-9].

Measurements of deuteron coalescence in high energy heavy ion collisions have been reported previously both at AGS energies [20–24] from 10 to 14.6 A·GeV/c and at SPS energies [25–29] at 200 or 158 A·GeV/c. Of these, the AGS results of Si+A [20] and Au+Au [22] collisions as well as the SPS results of Ref. [25] are of special importance for the present study because they also deal with the systematics of deuteron production as function of rapidity, centrality, mass and transverse mass. The data reported in Refs. [26–28] are preliminary versions of part of the presently reported results.

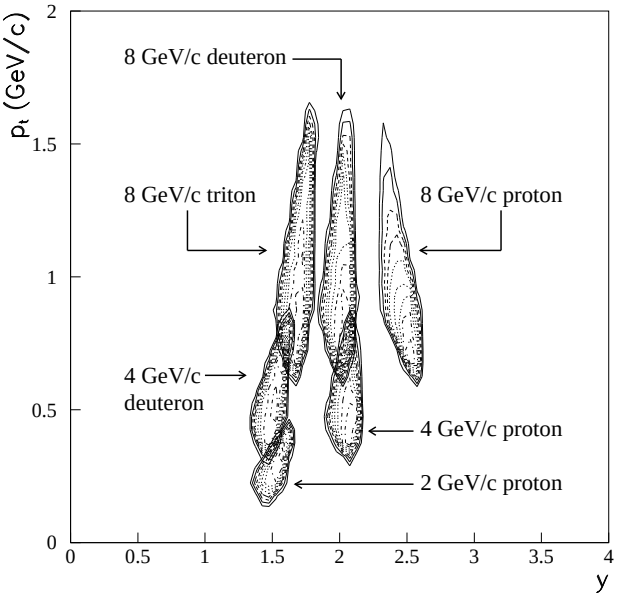

Fig. 1. The acceptance of the NA44 spectrometer at a polar angle of 129 mrad with respect to the beam direction. The acceptances are shown in p_t and y space for three different magnetic field settings correponding to average momenta of 8, 4 and 2 GeV/c, for protons (all three settings), deuterons (8 and 4 GeV/c) and tritons (8 GeV/c).

The paper is organised as follows: Sections 2 and 3 present the necessary experimental details and the data, respectively. In sect. 4 we present the mass systematics of single particle inverse slopes, while sect. 5 is devoted to the derivation of the B_A-values from the measurements and a presentation of their systematic trends with m_t, rapidity and centrality. Sect. 6 deals with an interpretation in terms of the models including flow quoted above and the conclusions are presented in the last section.

2 Experiment and data analysis

The data were measured with the NA44 magnetic spectrometer [10] using 158 A·GeV/c ^{208}Pb or 200 A· GeV/c ^{32}S ions from the CERN SPS accelerator. For Pb+Pb reactions protons, deuterons and tritons were measured at magnetic field settings corresponding to mean momenta of 8 GeV/c, protons and deuterons at momenta of 4 GeV/c and finally protons at 2 GeV/c, all at a polar angle relative to the beam direction of 129 mrad. The corresponding acceptances in $p_t - y$ (transverse momentum and rapidity) space are shown in Fig. 1, and are also quoted in Table 1, as $m_t - m$ and y intervals (m_t is the transverse mass $m_t = (p_t^2 + m^2)^{1/2}$and m the mass). It may be seen that the deuteron and proton data are in identical rapidity intervals while the tritons (8 GeV/c) are in an interval that lies 0.1 units higher than the 2 GeV/c protons. In the

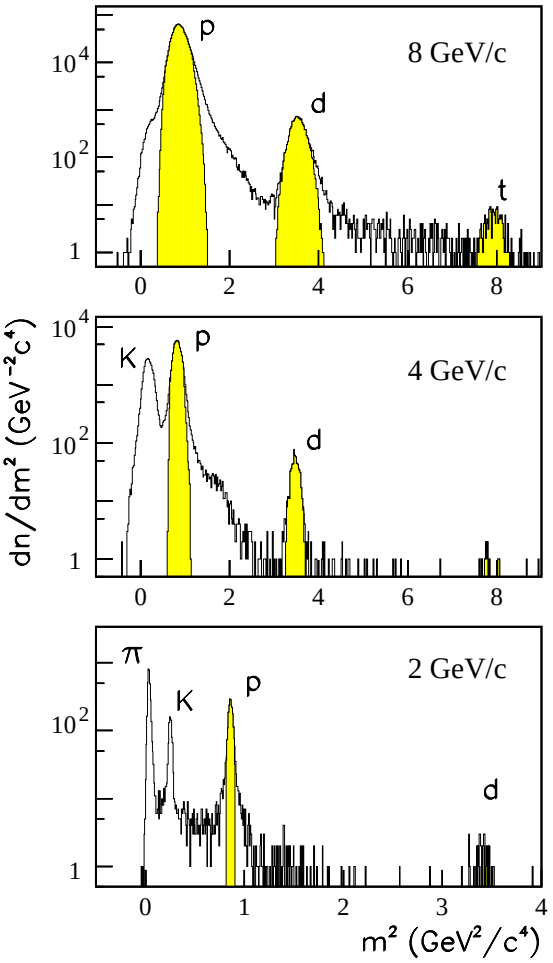

Fig. 2. Spectra of number of counts per unit of mass squared plotted against the mass squared. The particle identification for protons, deuterons and tritons are shown as shaded areas, corresponding to Gaussian fits. No global background subtractions were employed.

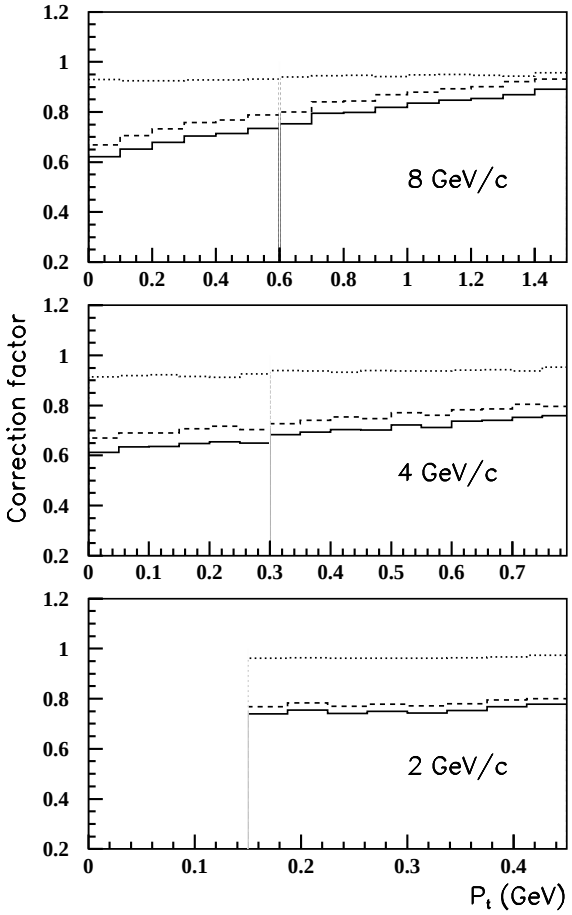

Fig. 3. The correction factor $C(p_t)$ from eq.(3), plotted against transverse momentum for the three magnetic field settings. The fully drawn curves incorporate both the Λ and Σ corrections, the dashed curves represent the corrections for Λ decays only and the dotted curves Σ decays only.

coalescence analysis to follow, this difference has been ignored. The quality of the particle identification made from the three time-of-flight measurements is demonstrated in Fig. 2.

The main trigger was provided by a scintillator (T_0) placed immediately behind the target, covering pseudo rapidities from 1.3 to 3.5. The offline centrality cuts were made from the additional information from a silicon-pad multiplicity detector placed after T_0 [10]. The cross section corresponding to the 20% of the reactions with highest charged particle multiplicity, was σ_{trig} ≈150 fm^2. A second level veto, for the rejection of pions and most of the kaons, was imposed on events with particles that fired the threshold Cherenkov counters in the spectrometer arm. The corresponding efficiency correction was measured from spectrometer runs with the Cherenkov veto turned off. All cuts in the data analysis were mimicked in the GEANT Monte Carlo simulation of the experiment and the corresponding efficiency corrections were applied to the data.

The Sulphur beam had a momentum of 200 A·GeV/c and the data were measured at the 8 GeV/c setting for deuterons and at 4 GeV/c for protons. The nominal spectrometer angles were 44 mrad and 129 mrad, the rapidity interval from 1.9 to 2.3 and the centrality 9% for S+S and 11% for S+Pb. The corresponding trigger cross sections were approximately 19 fm^2 for S+S and 44 fm^2 for S+Pb. The data analysis procedures were the same as used for the Pb beam measurements.

A special correction must be applied to the measured proton spectra, because the NA44 spectrometer does not measure the vertex from where the particles emerge. A number of protons originate as decay products from hyperons, e.g. from the decay $\Lambda \rightarrow p + \pi^-$, where the Λ in turn may have been produced from other hyperons, typically via $\Sigma^0 \rightarrow \Lambda + \gamma$, or from proton decay of other hyperons. The "feed down" corrections, $C(p_t)$, were calculated from the GEANT Monte Carlo simulation of the NA44

experiment, with particle distributions from the RQMD 1.08 [11] event generator as input,

$$C(p_t) = \frac{N_p(p_t)}{N_p(p_t) + N_\Lambda(p_t) + N_{\Sigma^+}(p_t)}, \qquad (3)$$

where N_p, N_Λ and N_{Σ^+} are the number of reconstructed direct protons, protons from $\Lambda + \Sigma^0$ decays and protons from Σ^+ decays, respectively. $C(p_t)$ for the Pb+Pb case is shown in Fig. 3 for the three momentum settings used, plotted versus p_t. The figure shows that the correction varies from 10% to 30% and that the high momentum setting exhibits a distinct p_t dependence. The RQMD model gives a fair account of the Λ cross sections measured by the NA49 and WA97 experiments [12,13] and the systematic errors introduced by the corrections of eq.(3) are considerably smaller than the corrections themselves.

3 Data and results

3.1 Pb+Pb

The invariant differential multiplicities Ed^3N/dp^3 for tritons, at the 8 GeV/c setting of the spectrometer are shown in Fig. 4 as function of $m_t - m$. Data are shown for the online multiplicity cut at 20% of the inelastic cross section, and in addition for an off-line multiplicity cut at 10%. The systematic errors on the multiplicities derive mainly from two sources, the trigger cross section and the live-time of the data acquisition system. For the data of Fig. 4, the total systematic error is estimated to be ≈10%.

The curves shown in the figure represent exponential fits to the data points of the functional form

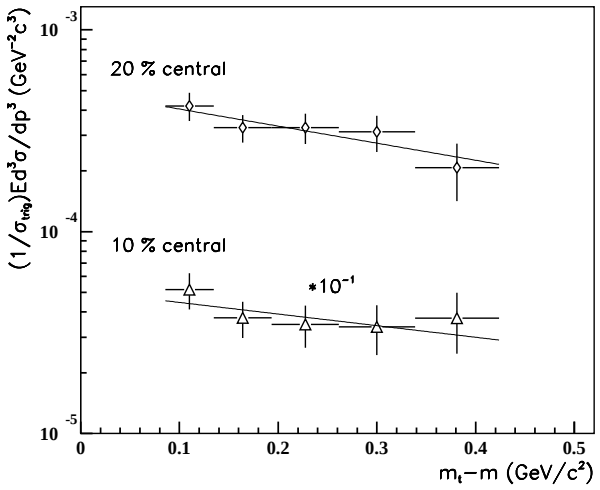

Fig. 4. Triton spectra from Pb+Pb interactions plotted as invariant triply differentiated multiplicity against transverse mass minus mass. The curves are exponential fits of the form shown in eq.(4). The fitted parameters are given in Table 1. The centrality cuts are descibed in the text. Only statistical uncertainties are shown.

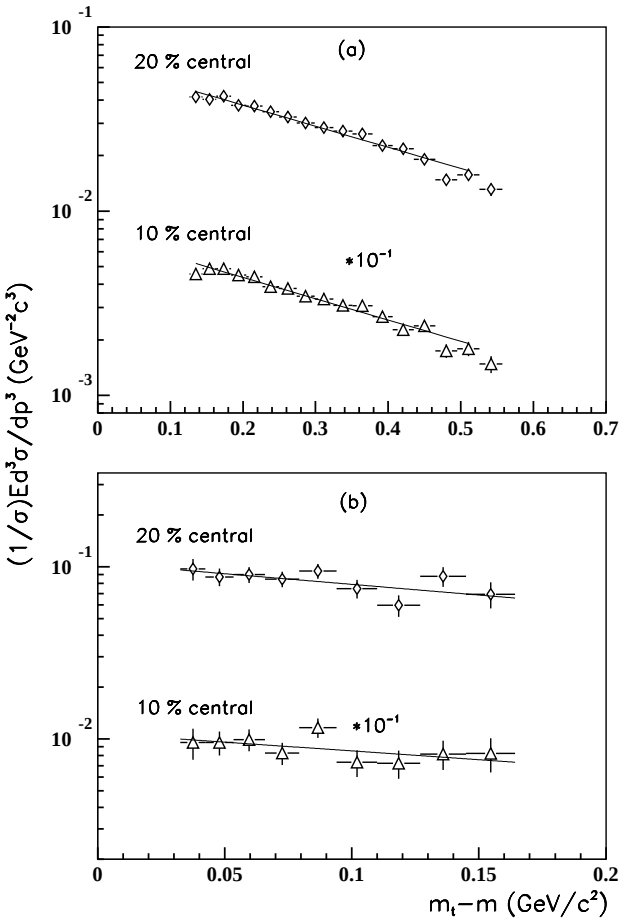

Fig. 5. Deuteron spectra from Pb+Pb collisions. (a) is for a magnetic field setting corresponding to a mean momentum of 8 GeV/c and a rapidity interval from 1.8 to 2.2, while (b) corresponds to a mean momentum of 4 GeV/c and rapidities from 1.4 to 1.7. Other details are as for Fig. 4.

$$Ed^3N/dp^3 = \frac{1}{\sigma_{trig}} E\frac{d^3\sigma}{dp^3} = A\exp(-(m_t - m)/T) \qquad (4)$$

with A and T as the fitting parameters. T is referred to as the inverse slope parameter. The $m_t - m$ interval used for the fit corresponds with the end points of the fit line shown in the figure.

Figs. 5 (a) and (b) depict the deuteron transverse mass spectra, (a) for the 8 GeV/c field setting and (b) for the 4 GeV/c setting. The exponential fits are shown in the same manner as for the tritons.

The proton spectra, corrected for "feed down", eq.(3), are shown in Figs. 6 (a), (b) and (c) for the three different field settings employed and for the two different cuts on charged multiplicity, 20% and 10%. The exponential curves have the same meaning as for tritons.

The rapidity density dn/dy may be obtained from the fitted exponential of eq.(4) by

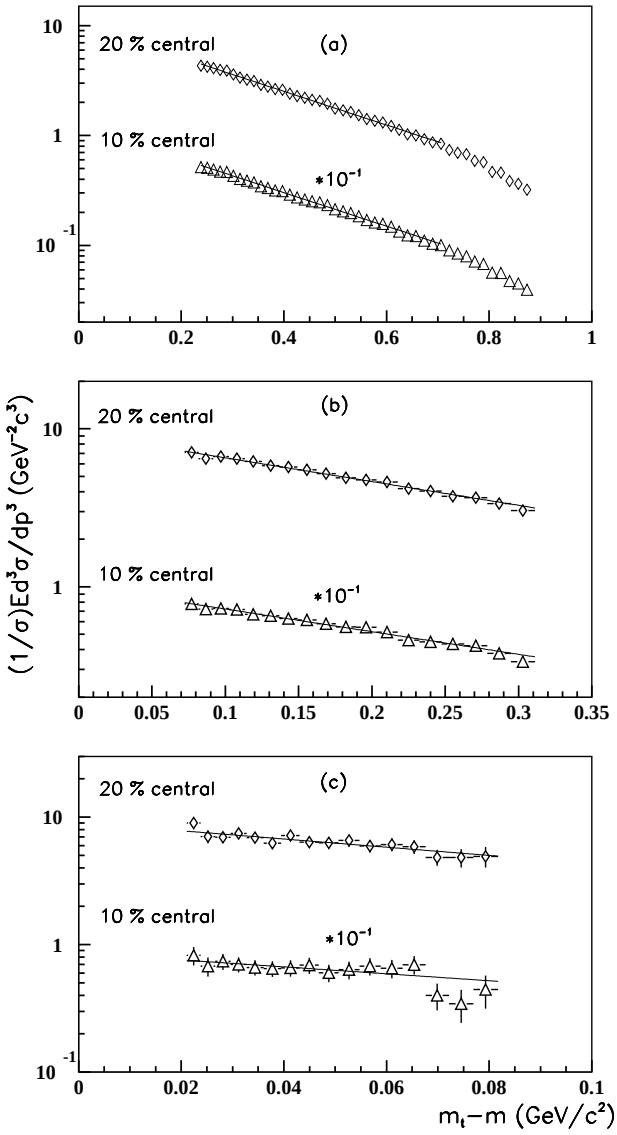

Fig. 6. Proton spectra from Pb+Pb reactions. (a) is for a mean momentum of 8 GeV/c and rapidities from 2.3 to 2.6, (b) corresponds to a mean momentum of 4 GeV/c and a rapidity interval from 1.8 to 2.2, while (c) is for 2 GeV/c and rapidities between 1.4 and 1.7. Other details are as for Fig. 4.

$$\frac{dn}{dy} = 2\pi \int_m^\infty \frac{1}{\sigma_{trig}} E \frac{d^3\sigma}{dp^3} m_t dm_t = 2\pi A T (T+m). \quad (5)$$

The values of dn/dy and T are collected in Table 1, which summarises the single particle results for the p, d and t spectra. The uncertainties listed in the table are statistical only. The dn/dy values represent extrapolations into unmeasured regions under the explicit assumption of exponential shape. Hence a strict systematic error cannot be assigned, but it is at least 10% from the normalisation and efficiency corrections as discussed above. For protons it is increased on account of the feed down corrections to about 15% . For the tritons, the m_t interval is very narrow and close to the rest mass, so the uncertainties on both dn/dy and the inverse slope become large and asymmetric. For the 10% centrality case the statistical uncertainty on dn/dy is larger than 100% and hence no dn/dy is quoted.

The inverse slope parameters, T, depend on which range of the data is fitted, because the data do not exactly follow the assumed functional form. For the proton data at 8 and 4 GeV/c the variations with fit range are larger than the statistical errors, typically 10-20 MeV. The deuteron spectra have similar systematic errors. For the 2 GeV protons the fitting range is critical and the m_t-m interval is close to zero, where the proton spectra often deviate from the exponential shape. Even if the statistical errors are large, the systematic errors may dominate. The extrapolated dn/dy values in this case are not representative and are not quoted in Table 1. In the triton and 2 GeV/c proton cases, the statistical uncertainties have been assigned from χ^2 contours and correspond to an increase of one unit in χ^2.

3.2 S+Pb and S+S

The deuteron and proton spectra from the S+S and S+Pb collisions are shown in Figs. 7 and 8, respectively. The exponential fits are shown in the same way as for the Pb+Pb data. The field settings were 8 GeV/c for the deuterons and 4 GeV/c for the protons and the rapidity interval covered from 1.9 to 2.3. The numerical results obtained from the exponential fits are shown in Table 1. The systematic uncertainties are similar to those quoted for the 8 GeV/c deuteron and 4 GeV/c proton results for Pb+Pb, i.e. 10% for deuteron dn/dy and ≈15% for protons and 10-20 MeV on the inverse slope parameters.

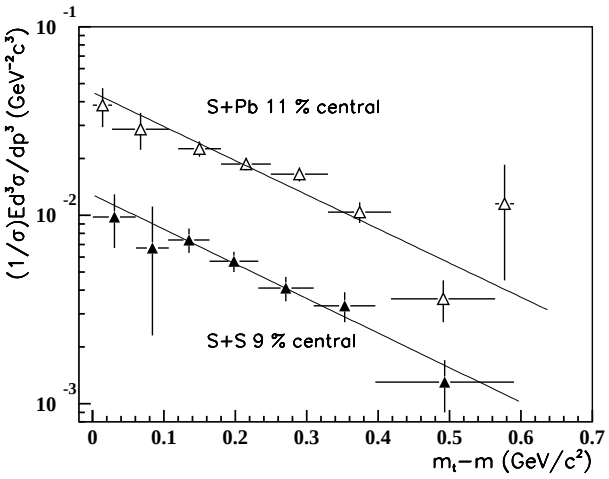

Fig. 7. Deuteron spectra from S+Pb and S+S collisions at 200 A·GeV/c beam momentum. Details are as for Fig. 4. See also Table 1 and the text.

Table 1. Single particle results. Errors are statistical only.

Reaction	Field setting	Centrality	A	Rapidity	m_t-m range	T (MeV)	dn/dy
Pb+Pb	8 GeV/c	20%	p	2.3-2.6	0.23-0.88	283±2	22.3±0.3
		10%	p	2.3-2.6	0.23-0.88	284±2	26.9±0.3
	4 GeV/c	20%	p	1.8-2.2	0.08-0.32	288±6	20.6±0.6
		10%	p	1.8-2.2	0.08-0.31	302±9	23.8±0.9
	2 GeV/c	20%	p	1.4-1.7	0.02-0.08	128±29	
		10%	p	1.4-1.7	0.02-0.08	114±33	
Pb+Pb	8 GeV/c	20%	d	1.8-2.2	0.13-0.56	379±13	0.34±0.02
		10%	d	1.8-2.2	0.13-0.56	376±17	0.39±0.02
	4 GeV/c	20%	d	1.4-1.7	0.03-0.16	350±149	0.51±0.23
		10%	d	1.4-1.7	0.03-0.16	425±286	0.66±0.46
Pb+Pb	8 GeV/c	20%	t	1.5-1.8	0.08-0.42	512^{+511}_{-179}	$0.0052^{+0.0047}_{-0.0013}$
		10%	t	1.5-1.8	0.08-0.42	$747^{+\infty}_{-380}$	
S+Pb	4 GeV/c	11%	p	1.9-2.3	0.01-0.32	200±4	10.6±0.1
	8 GeV/c	11%	d	1.9-2.3	0.02-0.58	240±20	0.14±0.01
S+S	4 GeV/c	9%	p	1.9-2.3	0.01-0.29	151±3	4.2±0.1
	8 GeV/c	9%	d	1.9-2.3	0.02-0.48	236±33	0.040±0.003

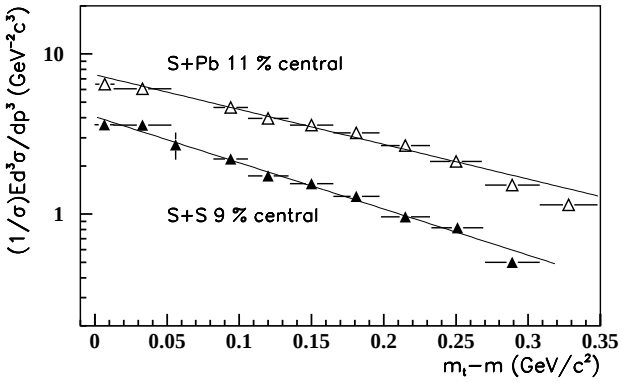

Fig. 8. Proton spectra from S+Pb and S+S collisions at 200 A·GeV/c beam momentum. Details are as for Fig. 4. See also Table 1 and the text.

4 Mass systematics of slope parameters

It has previously [14,25] been pointed out that the inverse slope parameters for Pb+Pb collisions depend systematically on the mass of the emitted particle: the inverse slope increases with increasing mass. This observation was interpreted as being caused by a collective transverse flow. The present measurements extend the mass range used in [14] by deuterons and tritons. The previous π and K meson results are shown in Fig. 9 as filled triangles together with the present results for 20% centrality (filled circles). The π and K results are for a centrality of 6.4%. The present p and d data for Pb+Pb collisions were also analysed with 5 and 2% centrality cuts, but no significant variation with centrality was observed for the inverse slope parameters. The K and π inverse slopes have also been measured at other centralities [15] without revealing any systematic changes. Inverse slopes, however, do depend sensitively on rapidity. The open points for π, K and p in figure 9 have been corrected by means of RQMD calculations to a common rapidity interval of $1.6< y <2.0$, corrections that are barely outside the statistical errors. The proton slopes are from spectra corrected for feed down, which is different from the proton slopes presented in [14] and [16].

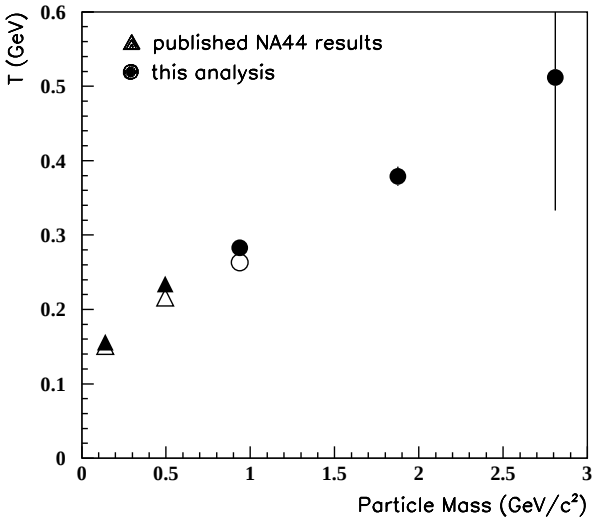

Fig. 9. Inverse slope parameters T (see eq.(4)) as a function of particle mass. The data for pions and kaons are from Ref. [14] while the proton, deuteron and triton results are from this work. Open points are data corrected by means of RQMD to a rapidity interval of $1.6< y <2.0$.

The previous observation of inverse slope parameters as increasing with increasing mass is further supported by the present data.

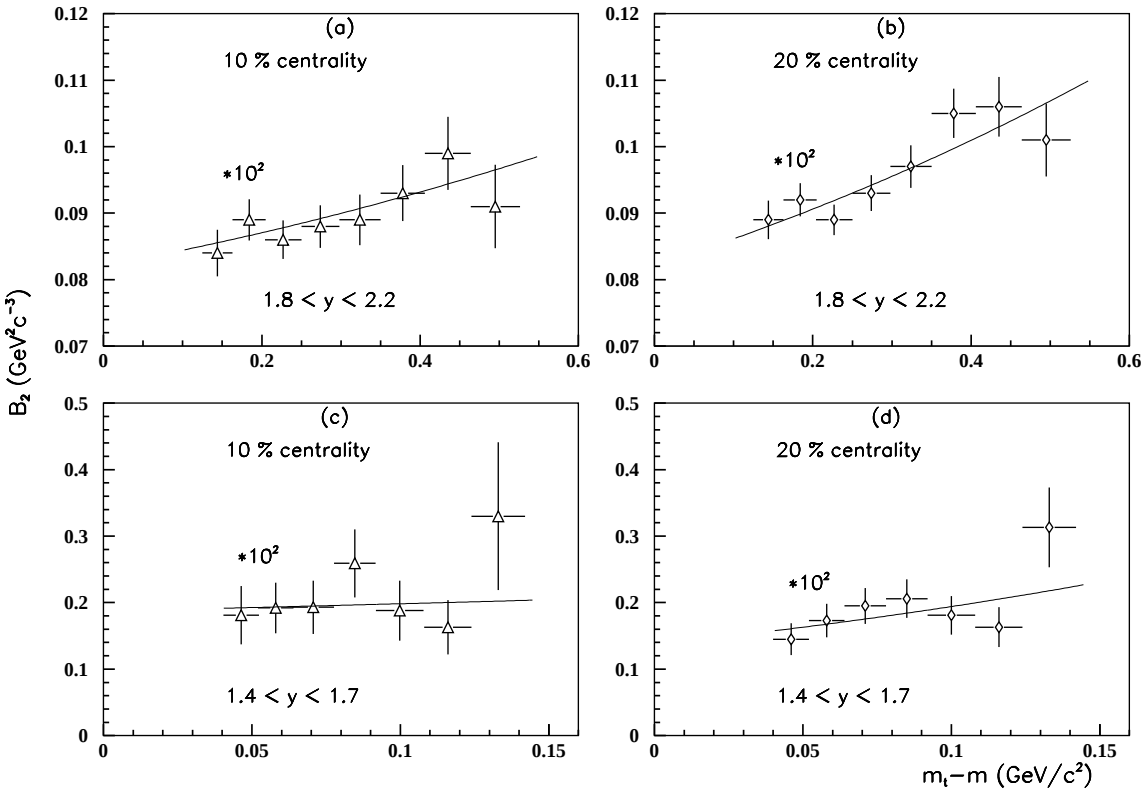

Fig. 10. B_2 values from Pb+Pb reaction plotted versus deuteron $m_t - m$. The two top frames (a and b) are from 8 GeV/c deuteron and 4 GeV/c proton data. All B_2 values have been multiplied by a factor 10^2. The curves through the measured points represent fits to eq.(10) and the fit parameters are given in Table 3. Only statistical uncertainties are shown. The two lower frames, (c) and (d), are from 4 GeV/c deuteron and 2 GeV/c proton data. All other details are as for the two top frames.

5 The coalescence analysis

The prescription eq.(1) has been used to derive B_2 and B_3 values from the spectra in Figs. 4-8. Fig. 10 shows Pb+Pb B_2-values versus deuteron $m_t - m$ for the rapidity interval from 1.8 to 2.2 (a and b), corresponding to deuterons from the 8 GeV/c and protons from the 4 GeV/c field settings, while Figs. 10 (c) and (d) depict B_2 values from Pb+Pb collisions at the 4 GeV/c deuteron setting and the 2 GeV/c proton setting in the rapidity interval $1.4< y <1.7$. The Pb+Pb B_3 from tritons at the 8 GeV/c and protons at 2 GeV/c settings in the rapidity interval 1.5 to 1.8 are presented in Fig. 11 and the S+S and S+Pb B_2-values are shown in Figs. 12. For all three figures the cluster $m_t - m$ was used as the abscissa.

The figures demonstrate that the B-values in general depend on m_t, a feature to be expected because of the differences in inverse slopes between the p, d and t spectra (see also [22,25]). To the extent that the single particle spectra can be represented by an exponential function in m_t, the B-values depend exponentially on the transverse mass of the cluster M_t,

$$B_A \propto \exp(M_t(1/T_p - 1/T_A)), \qquad (6)$$

where T_p is the inverse slope of the proton spectrum and T_A the inverse slope for the cluster spectrum. (The notation M_t is used from now on for the transverse mass of the cluster, while m_t denotes the same quantity for a nucleon; similarly M and m denote the cluster and nucleon rest masses, respectively.) The coalescence parameters are summarised in Table 2 in two ways: For each rapidity interval the weighted average B_A is given for the $M_t - M$ range of the measurement (see Figs. 10-12); in addition the parameters of exponential fits to the functional form

$$B_A = a \exp(b(M_t - M)) \qquad (7)$$

are given in the two right hand columns. Note that both a and b were allowed to vary in the fitting procedure, so b does not necessarily equal the difference in inverse slope values from Table 1.

It appears from the average B_A-values in the table, that the dependence on centrality is weak. In most cases B_A increases with increasing M_t. This (see eq.(6)) reflects that $T_A > T_p$ in accordance with the systematics of section 4. In the two cases, where an increase with $m_t - m$ is not observed (Pb+Pb deuterons for $1.4< y <1.7$ and S+Pb deuterons $1.9< y <2.3$) the B_2 values do not vary with $m_t - m$.

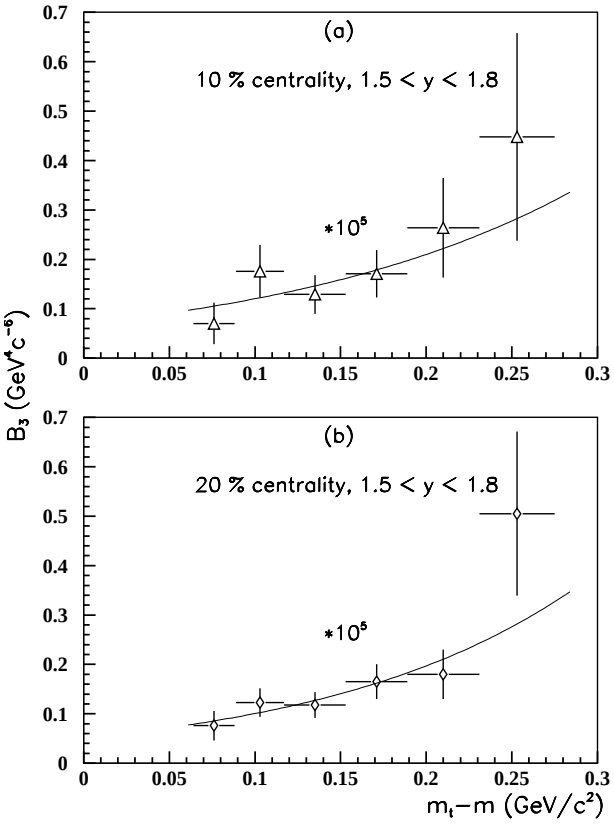

Fig. 11. B_3 values from Pb+Pb collisions plotted versus triton $m_t - m$. The results are from 8 GeV/c tritons and 2 GeV/c protons. All data have been multiplied by a factor of 10^5. The curves are from fits to eq.(13) as explained in the text and the fit parameters are stated in Table 3. All other details are as in Fig. 10.

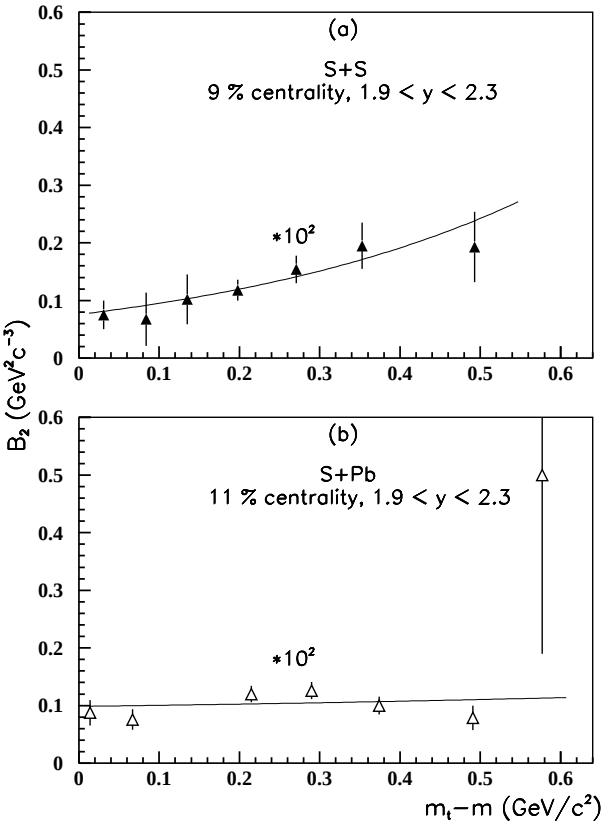

Fig. 12. B_2 values from S+S and S+Pb interactions at 200 A·GeV/c beam momentum. All details are as for Fig. 10.

In the thermal limit, where the interpretation of B-values in terms of eq.(2) becomes valid, both M_t and rapidity dependences become explicit. In the Boltzmann limit one has

$$B_A \propto \frac{1}{(M_t \cosh y)^{A-1}}, \qquad (8)$$

where y is the common rapidity of protons and cluster in the source system of reference. The general trend with M_t from the inverse slope parameters in Table 1 and from Figs. 10-12 is an increase in B_A with increasing M_t rather than a decrease as suggested by eq.(8). The fit parameters b quoted in Table 2 are positive in all cases, but only for Pb+Pb in the rapidity interval from 1.8 to 2.2 and for S+S are they positive by two standard deviations.

It appears from Table 2 that the average values of B_2 for the Pb+Pb system depend on rapidity: the B_2-value doubles from the 1.8-2.2 rapidity interval to the 1.4-1.7 interval. Eq.(8) predicts a decrease by a factor of ≈1.5 if we take the source rest system to be the center of mass system for Pb+Pb at y=2.91.

6 Discussion

In the Au+Au experiment at 11.6 A·GeV/c reported in Ref. [22] the B_2-values were also observed systematically to increase with m_t and to increase in magnitude towards mid-rapidity. The Si+A experiment at 14.6 A·GeV/c shows that B_2 decreases with target mass, averaged over m_t. The SPS Pb+Pb experiment [25] again demonstrates that B_2 increases with increasing m_t, here for the rapidity interval 2.0< y <2.5. For this rapidity interval the B_2-value averaged over the same $m_t - m$ range as used in the present experiment is 5.7±1.5 GeV^{2}c^{-3}, i.e. somewhat smaller than the present value of 8.8±0.1 Gev^{2}c^{-3} for 1.8< y <2.2. The increase in B_2 with increasing m_t apparently is a general phenomenon, whereas the rapidity dependence at 11.6 A·GeV/c is in the opposite direction of the observations for Pb+Pb at 158 A·GeV/c.

It does not seem reasonable to interpret the B_A-values in terms of the thermal expression of eq.(2) in view of the systematics of the data presented in the previous section. In general one should expect the dynamics of the source expansion to be important for the coalescence mechanism, and the following discussion is therefore based on models that explicitly consider rapid source expansion.

Table 2. B_A-values in $(\mathrm{GeV^2c^{-3}})^{A-1}$

Reaction	A	Rapidity	Centrality %	B_A $\cdot 10^{-4}$	a $\cdot 10^{-4}$	b
Pb+Pb	2	1.8-2.2	20	9.35±0.11	8.1±0.3	0.55±0.29
Pb+Pb		1.8-2.2	10	8.84±0.13	8.1±0.4	0.33±0.15
Pb+Pb		1.4-1.7	20	18.00±1.10	13.7±3.2	3.50±2.70
Pb+Pb		1.4-1.7	10	19.60±1.70	18.7±6.7	0.56±4.10
Pb+Pb	3	1.5-1.8	20	0.013±0.002	0.0048±0.0027	7.1±3.4
Pb+Pb		1.5-1.8	10	0.014±0.002	0.0047±0.0013	8.2±2.4
S+Pb	2	1.9-2.3	10	10.30±0.70	9.8±1.2	0.20±0.36
S+S	2	1.9-2.3	9	12.10±1.10	7.5±1.5	2.34±0.72

The models of Polleri et al. and of Scheibl and Heinz [8,9] incorporate a fast "collective" expansion and a local thermodynamic equilibrium, so the observed inverse slopes in the transverse spectra (Fig.9) are interpreted as an apparent temperature, comprised of a local temperature and the superimposed "collective" motion. The coalescence process is described in the local equilibrium system and it is shown by Scheibl and Heinz that the observed nucleon and cluster spectra as well as the B_A-values can be understood in terms of the same lengths of homogeneity that can be extracted from HBT interferometry. The term "lengths of homogeneity", used in Ref. [9], stands for the radius parameters extracted from interferometry; the term "volume of homogeneity" is used for a product of three such radius parameters, as defined more precisely in eq.(9) below.

The model of Polleri et al. only deals with the transverse motion, while Scheibl and Heinz also include the motion in the beam direction.

A preliminary version of the Pb+Pb data presented in Figs. 6 and 5 for 20% centrality and rapidity interval 1.8-2.2 were used by Polleri et al. [8] to calculate a set of dimensionless transverse density functions, one for each "local" temperature assumed. The coalescence condition of proportionality between the deuteron and the square of the proton densities, was then used to construct a collective transverse velocity profile. The various combinations of "local" temperature and density profile all fit the experimental spectra about equally well. In the thesis of Polleri [7] the corresponding triton results are also calculated, assuming two competing routes, namely a direct "triple" coalescence p+n+n→t and a sequential coalescence p+n+n →d+n→t. The predicted triton spectra again fit the data for all the density and temperature combinations used from the p and d spectra. Without the sequential route, however, the triton cross section is severely underpredicted.

If the value of the local temperature is taken to be 130 MeV (see e.g. Refs. [9,15]) the result of the analysis in Ref. [8] may be summarised as a transverse velocity profile and a local proton (or deuteron) density as function of transverse distance. The root mean square velocity is ≈0.4c and the root mean square transverse radius ≈8.1 fm (interpolated from Table 1 of Ref. [8]). The transverse density profile is more box-like than Gaussian in shape. An important further test of this model would be a consistent description of the present B_2 results in the rapidity interval from 1.4-1.7.

The model of Scheibl and Heinz [9] assumes a boxlike transverse density profile and results in a connection between the B_2-value and a volume of homogeneity given by

$$B_2 = e^{\frac{N(\mu_n-\mu_p)}{T}} \frac{3\pi^{3/2} < C_d > \hbar^3}{M_t R_\perp^2(M_t) R_\parallel(M_t)} e^{(M_t-M)(1/T_p - 1/T_d)}, \quad (9)$$

where μ are the chemical potentials for protons and neutrons, $< C_d >$ is a quantum mechanical correction factor related to the deuteron internal structure and $R_\perp$ and $R_\parallel$ denote lengths of homogeneity, while the product $R_\perp^2 R_\parallel$ is the volume of homogeneity mentioned above. The formula above combines equations (6.4) and (6.5) in Ref. [9], where it should be noted that the transverse and rest masses in eq.(9) refer to the deuteron, while the nucleon masses were used in Ref. [9].

The B_2-value for antideuterons has been measured [17] in Pb+Pb collisions at 10% centrality for a rapidity interval from 1.9 to 2.1 and an antideuteron $M_t - M$ interval from 0.16 to 0.53 GeV with a value of $(4.4\pm1.3\pm1.8)10^{-4}$ $\mathrm{GeV^2c^{-3}}$ averaged over M_t. The second quoted uncertainty represents an estimate of the systematic uncertainty of the correction for the contribution from weak decays to the antiproton yield. The comparable deuteron B_2-value from Table 2 is $(8.8\pm0.1\pm0.9)10^{-4}$ $\mathrm{GeV^2c^{-3}}$. With a ratio $B_2/B_{\bar{2}} \approx 2$, the difference between the chemical potentials is $\mu_n - \mu_p = 0.00036$ GeV with a near 100% uncertainty. In this estimate the "local" temperature was set to 130 MeV and neutron number N=126 and the slope factors were assumed to be equal for particles and antiparticles. It is noted that, if a 5 to 10% centrality cut in the $\bar{d}$ case had been used instead of 0 to 10%, the B_2-values for deuterons and antideuterons would have been very close ($9.8\cdot 10^{-4}$ for antideuterons and no change for deuterons). The data are thus in agreement with $\mu_p = \mu_n$ in eq.(9).

Eq.(9) was used to derive volumes of homogeneity in the form of $R_\perp^2 R_\parallel$ values in $\mathrm{fm^3}$. The expression

$$B_2 = \alpha \frac{1}{M_t} \exp((M_t - M)\delta) \quad (10)$$

Table 3. Volumes of homogeneity

Reaction	A	Rapidity	Centrality %	α $\cdot 10^{-4}$	δ	$< C_A >$	$R_\perp^2 R_\parallel$ fm^3
Pb+Pb	d	1.8-2.2	20	15.4±0.5	1.0±0.1	0.80	68±2
Pb+Pb	d	1.8-2.2	10	15.4±0.7	0.8±0.2	0.80	67±3
Pb+Pb	d	1.4-1.7	20	25.7±6.0	4.0±2.7	0.80	40±9
Pb+Pb	d	1.4-1.7	10	35.1±12.5	1.1±4.2	0.80	29±10
S+Pb	d	1.9-2.3	11	18.5±2.6	0.7±0.5	0.61	42±6
S+S	d	1.9-2.3	9	14.2±2.3	2.8±0.6	0.55	50±8
Pb+Pb	t	1.5-1.8	20	0.038±0.004	1/0.128	0.70	59±3
Pb+Pb	t	1.5-1.8	10	0.037±0.006	1/0.114	0.70	60±4
Pb+Pb	π-HBT	2.5-3.1	15				76±9
Pb+Pb	π-HBT		5				83±21

The two last lines are HBT results from Refs. [10,19]

was fitted to the B_2-values of Figs. 10 and 12 with α and δ as the fit parameters and M_t and M referring to the deuteron. (The fits are shown in the figures in comparison with the data). The volume of homogeneity is then

$$R_\perp^2 R_\parallel = \frac{0.1283 < C_d >}{\alpha}. \tag{11}$$

The $< C_d >$ is 0.80 for the Pb+Pb case (see Ref. [9]) and for the sulphur beam cases it was roughly estimated from eq.(4.12) of Ref. [9] by scaling the R-values for Pb+Pb in the quoted reference to S+Pb and S+S with the values of Table 4 in Bearden et al. [18]. The $< C_d >$ are given in the table, as are the volumes of homogeneity from HBT results for Pb+Pb from NA44 [10] and NA49 [19], the latter as quoted in Ref. [9]. The HBT-values are from pion data at m_t-values near 1 GeV and from higher rapidities than the present coalescence data.

The main result from the analysis of Table 3, is that the present Pb+Pb data in the rapidity range from 1.8-2.2 yield volumes of homogeneity in near agreement with the HBT results but give lower values for the more backward rapidity interval from 1.4-1.7. The HBT pion-pair m_t range used for the comparison is important. The fit parameter α used to determine the value of the volume of homogeneity corresponds to setting $M_t = M$, i.e. corresponds to a nucleon m_t value of 0.94 GeV. One should use a similar pion-pair m_t value in the HBT case (see also Ref. [9]). The HBT results used in Table 3 are for m_t values near the nucleon mass. If lower HBT m_t values are used in the comparison, the HBT volumes become considerably larger and the agreement disappears.

The relation between B_3 and the volume of homogeneity, corresponding to eq.(9) is

$$B_3 = \frac{18\pi^3 < C_t > \hbar^6}{\sqrt{3} M_t^2 R_\perp^4 R_\parallel^2} e^{(M_t - M)(1/T_p - 1/T_t)} \tag{12}$$

with the proton and neutron chemical potentials set equal to one another. The inverse slope parameters for the tritons T_t are ill defined, but they are considerably larger than T_p (Table 1) and have been ignored in fitting eq.(12). The volume of homogeneity was then found by fitting α in the expression

$$B_3 = \alpha \frac{1}{M_t^2} \exp((M_t - M)/T_p) \tag{13}$$

to the data (see Fig. 11) with the relation

$$R_\perp^2 R_\parallel = (\frac{0.01901 < C_t >}{\alpha})^{\frac{1}{2}}. \tag{14}$$

The values for T_p were from Table 1 at a field setting of 2 GeV/c, and the quantum mechanical correction factor related to the triton internal structure is C_t=0.70 according to Ref. [9]. The α-values as well as the volumes of homogeneity are quoted in Table 3, where the value for the parameter δ is $1/T_p$ from Table 1 and has not been fitted. The uncertainties quoted on the volumes of homogeneity are those from the fitting procedure only, and do not include any systematic uncertainties. In the triton case the two most important sources of systematic uncertainties, are the feed down corrections and the use of a fixed value for T_p. The feed down corrections enter in the power $\frac{3}{2}$ in the derived volume and the derived α value depends sensitively on T_p. The uncertainties quoted in Table 1 for T_p corresponds to a 20% uncertainty on the derived volume. Typical values for the systematic uncertainties are 20% for volumes derived from deuterons and 30% for the triton volumes. It should also be pointed out, that the T_p values come from fitting the proton spectra at very small $m_t - m$ values (0.02-0.05 GeV/c^2) and probably are not characteristic of the spectra as a whole. The triton volumes in the rapidity interval 1.5-1.8 are somewhat larger than the deuteron volumes in the 1.4-1.7 interval. The systematic uncertainty from the feed down corrections is unimportant in this comparison, but the uncertainty from T_p remains, so the differences are less than two standard deviations. There is no demonstrated need for introducing a second composite route in the triton formation (p+n+n→d+n→t) in order to obtain similar volumes of homogeneity for deuterons and tritons.

7 Conclusions

The measurements cover deuteron coalescence for three different collision systems, Pb+Pb, S+Pb and S+S, and triton coalescence for the Pb+Pb system. Both deuteron and triton measurements exhibit a dependence on the cluster transverse mass M_t that yields B_A-values which increase with increasing M_t. The deuteron measurements from Pb+Pb show a rapidity dependence opposite of that expected from the single (spherical) source model without expansion. No systematic dependence of the derived B_A-values on centrality was found.

The main source of systematic uncertainties stem from corrections to the observed proton spectra for feed down from hyperon decays, and these uncertainties tend to dominate over the statistical uncertainties.

The interpretation of the measured cross sections for protons, deuterons and tritons in terms of interaction volumes were based on theoretical models ([8,9]) that explicitly include the effects of collective expansion.

When the Pb+Pb B_2-values in the rapidity interval from 1.8-2.3 are interpreted in the framework of Scheibl and Heinz (Ref. [9]) the resulting volumes of homogeneity agree with those from HBT measurements when the pion pair m_t is close to the nucleon mass. The deuteron Pb+Pb volumes of homogeneity depend markedly on rapidity, a feature that disagrees with the model of Ref. [9]. The volumes derived for the S collisions are smaller than the Pb+Pb volumes in the same rapidity interval at the two sigma level, ignoring systematic uncertainties.

The Pb+Pb B_3-values yield volumes of homogeneity that lie between the corresponding volumes from deuterons in the two rapidity ranges covered. Compared to the deuteron volume in the rapidity interval from 1.4-1.7, that is close to the interval for the triton measurements, the triton volume is larger than the deuteron volume, but the difference does not reach a two sigma significance. Thus the Scheibl and Heinz model does not require any substantial contribution to the triton formation from intermediate deuteron formation in contrast to the conclusion drawn by Polleri [7] from comparisons to a preliminary version of the present data.

Acknowledgements The NA44 collaboration wishes to thank the staff of the CERN PS-SPS accelerator complex for their excellent service in providing the heavy ion beams. We acknowledge many useful discussions with A. Polleri and Raffaele Mattiello. We are grateful for the financial support given by the Danish Natural Science Research Council, the Japanese Society for the Promotion of Science, the Ministry of Education, Science and Culture of Japan, the Swedish Research Council, the Fond für Förderung der Wissenschaftlichen Forschung, Austria, the National Science Foundation, USA and the U.S. Department of Energy. One of us (OH) thanks the Danish Natural Science Research Council for a special grant and the TRIUMF laboratory in Vancouver, B.C., Canada for hospitality during the preparation of parts of this work.

References

1. S.T. Butler and C.A. Pearson, Phys. Rev. **129**, 836 (1963)
2. A. Schwarzschild and C. Zupancic, Phys. Rev. **129**, 854 (1963)
3. L.P. Csernai and J.I. Kapusta, Phys. Rep. **131**, 223 (1986)
4. A.Z. Mekjian, Phys. Rev. **C17**, 1051 (1978)
5. W.J. Llope et al., Phys. Rev. **C52**, 2004 (1995)
6. A. Polleri, J.P. Bondorf and I.N. Mishustin, Phys. Lett. **B419**, 19 (1998)
7. A. Polleri, Ph.D. Dissertation, Faculty of Science, University of Copenhagen (1999)
8. A.Polleri et al., Phys. Lett. **B473**, 193 (2000)
9. R. Scheibl and U. Heinz, Phys. Rev. **C59**, 1585 (1999)
10. I.G. Bearden et al., The NA44 collaboration, Phys. Rev. **C58**, 1656 (1998)
11. H. Sorge, Phys. Rev. **C52**, 3291 (1995)
12. H. Appelhäuser et el.,The NA49 collaboration, Nucl. Phys. **A638**, 91c (1998)
13. E. Andersen et al., The WA97 collaboration, Phys. Lett. **B449**, 401 (1999)
14. I.G. Bearden et al., The NA44 collaboration, Phys. Rev. Lett. **78**, 2080 (1997)
15. I.G. Bearden et al., The NA44 collaboration, Phys. Lett. **B471**, 6 (1999)
16. I.G. Bearden et al., The NA44 collaboration, Phys. Lett. **B388**, 431 (1996)
17. I.G. Bearden et al., The NA44 collaboration, Phys. Rev. Lett. **85**, 2681 (2000)
18. I.G. Bearden et el., The Na44 collaboration, Eur. Phys. J. **C18**, 317 (2000)
19. H. Appelhäuser et al., NA49 Collaboration, Eur. Phys. J. **C2**, 661 (1998)
20. T. Abbott et al., The E802 Collaboration, Phys. Rev. **C50**, 1024 (1994)
21. J. Barette et al., The E814 Collaboration, Phys. Rev. **C50**, 1077 (1994)
22. L. Ahle et al., The E802 Collaboration, Phys. Rev. **C60**, 064901 (1999)
23. L. Ahle et al., The E802 Collaboration, Phys. Rev. **C55**, 2604 (1997)
24. L. Ahle et al., The E802 Collaboration, Phys. Rev. **C57**, 1416 (1998)
25. S.V. Afansiev et al., The NA49 Collaboration, Phys. Lett. **B486**, 22 (2000)
26. A. Sakaguchi et al., The NA44 Collaboration, Nucl. Phys. **A638**, 103c (1998)
27. J. Simon-Gillo et al., The NA44 Collaboration, Nucl. Phys. **A590**, 483c (1995)
28. A.G. Hansen et al., The NA44 Collaboration, Nucl. Phys. **A661**, 387c (1999)
29. G. Ambrosini et al., The NA52 Collaboration, New Journ. of Physics **1**, 22.1 (1999)